MELANOMA DETECTION

by

RASHIKA AGARWAL	20BCE1342
POULAMI BERA	20BCE1305
MIZBA K	20BCE1004

A project report submitted to

JAGADESH KANAN

SCHOOL OF COMPUTER SCIENCE ENGINEERING

in partial fulfilment of the requirements for the course of

CSE4019– IMAGE PROCESSING

in

B. Tech. COMPUTER SCIENCE ENGINEERING

VIT®
Vellore Institute of Technology
(Deemed to be University under section 3 of UGC Act, 1956)

Vandalur – Kelambakkam Road

Chennai – 600127

APRIL-2020

TABLE OF CONTENTS

8 ROLES

ABSTRACT

Skin cancer that spreads rapidly, such as melanoma, has a significant death risk if it is not detected early and treated. Accurately identifying skin cancer at an early stage can save the patients' lives. A prompt and accurate diagnosis can improve the patient's chances of survival. The creation of a computer-aided diagnostic support system is required. Using MobileNetV2, this study suggests a unique deep transfer learning model for categorising melanoma. A deep convolutional neural network called MobileNetV2 categorises the sample skin lesions as benign or malignant. Using the ISIC 2020 dataset, the suggested deep learning model's effectiveness is assessed. Less than 2% of the samples in the dataset are cancerous, which worsens the class disparity. To address the class imbalance issue and add diversity to the dataset, a variety of data augmentation strategies were used. The experimental findings show that, in terms of accuracy and computing cost, the suggested deep learning technique performs better than cutting-edge deep learning algorithms.

KEYWORDS-:

Deep learning; skin cancer; malignant melanoma; ISIC-2020 dataset; MobileNetV2

INTRODUCTION

Skin cancer is the uncontrolled growth of abnormal skin cells that results in malignant tumours. Unprotected skin exposure to ultraviolet (UV) radiation is the primary aetiology of the majority of these cancers. Melanomas make up just 1% of all skin cancers, with basal cell carcinoma and squamous cell carcinoma making up the remaining 99%. It is a terrible illness that is among the most prevalent in American society. Every year, more than five million different cases of skin diseases are recorded in just the United States. Skin cancer has been steadily increasing for decades. The most deadly form of skin cancer, melanoma now accounts for over 75% of skin cancer fatalities. According to the American Cancer Society, there will be approximately 99,780 new instances of melanoma found in 2022, with roughly 57,100 men's cases and 42,600 women's cases being recorded. About 7650 people are anticipated to pass away from melanoma. Melanocytes are impacted by melanoma (squamons cell layer). It may be further split into benign and malignant categories depending on the aggressiveness of the cancerous cells. A mole or tag that doesn't contain malignant cells is referred to as a benign skin lesion. Due to the high number of cancer cells present in malignant lesions, prompt medical attention is required. Current statistics indicate that if melanoma is found before it spreads close to lymph nodes, the survival probability is 99%. If melanoma spreads near lymph nodes, the survival percentage is approximately 68%; if it spreads near lymph nodes and other organs, the survival rate is approximately 30%. According to the statistics, 1,361,282 persons had melanoma as of 2019. A total of 324,635 persons were diagnosed with melanoma in 2020, and 57,043 of them passed away from the disease.

Skin cancer can be found in many different ways by doctors. A skilled dermatologist often performs a battery of tests, starting with the naked eye detection of suspected tumours, followed by dermoscopy, and then a biopsy. It could take a while, and the person might move on to a later stage. With an absolute accuracy range of 75% to 84%, dermoscopic image detection performance has risen by 50%. Moreover, accurate diagnosis is distinct and heavily dependent on the skills of the clinician. Skin illness manual diagnosis is exceedingly difficult and taxing for the patient. Because computer-assisted diagnosis aids medical professionals in reviewing dermoscopy procedures in cases where there is a shortage of professional availability or diagnostic competence. A method for reducing inter- and intra-variability is computer-based classification. Modern computer-assisted dermatological image categorization systems suffer from two fundamental flaws: insufficient data, and the imaging process itself, which relies on a special device called a dermoscopy to obtain skin images, as opposed to other medical images like biopsy and histology images, which are obtained using a biopsy and microscope. The most recent methods required intensive preprocessing, segmentation, and feature extraction procedures to classify skin pictures.

The transformation brought about by adding technology to every aspect of our existence is analogous to that brought about by artificial intelligence, which is a novel field. By eliminating the need for human feature extraction, machine learning (ML) techniques facilitate effective categorization tasks. Using ML techniques to aid in precise cancer detection has recently attracted increasing attention. Over the past two decades, machine learning algorithms have considerably improved cancer prediction accuracy by 15% to 20%. Due to its wide range of applications, deep learning is one of AI's most quickly expanding subjects. Convolutional neural networks (CNNs) are one of the most effective and well-liked machine learning (ML) algorithms for picture identification and classification and have been used to classify skin lesions. CNNs are powered by complex computer techniques and large datasets. Traditional ML approaches used to classify images no longer require the preliminary data or intricate picture preprocessing techniques. Dermatologists and some deep-learning-based classifiers have both shown that they can accurately classify skin cancer photos. CNNs can therefore aid in the creation of dermatologist-level computer-aided fast skin lesion classifiers.

Nevertheless, there are still few training datasets for high-quality medical imaging. It primarily has to do with the lack of photos for aberrant classes that have been annotated or labelled. For small training datasets, CNNs with basic design are more prone to overfit. Some researchers employ incredibly complex CNNs models (Resnet152, for example, has 152 layers). Although this boosts computational costs and network classification performance, it is a significant issue for clinical applications. Moreover, pre-trained CNNs are being used by researchers to categorise skin lesions, which avoids the overfitting problem and makes use of features discovered from real-world picture datasets (such as ImageNet).

Based on MobileNetV2, the current work suggests a deep transfer learning method for classifying melanoma. Pre-processing and substantial augmentation techniques are utilised for the initial stage of melanoma detection and recognition in order to solve the imbalanced class problem in the ISIC-2020 challenge dataset. The transfer learning MobileNetV2 architecture is utilised in the second stage to automatically extract features and classify them as benign or malignant.

LITERARTURE SURVEY

The last ten years have seen a rise in interest in deep learning [1,2,3]. The classification of diseases has made extensive use of convolutional neural networks [4,5]. Insufficient training samples in datasets make it difficult to train CNN architectures. In order to deal with a new dataset with a variable spatial resolution, a varied number of bands, and fluctuation in the signal-to-noise ratio, a partial transferable CNN was suggested in [14]. With fewer training samples, partial CNN transfer with even-numbered layers improves mapping accuracy for the target dataset, according to experimental results employing several state-of-the-art models. [15] proposes a novel approach employing transfer learning to handle multi-resolution images from diverse sensors. The trained weights from CNN's training on a common image data set were applied to other data sets with various resolutions. Initially, there were just two classifications for skin cancer diseases: benign and malignant. Machine learning algorithms like K-Means and SVM were used by Canziani et al. [6] to reach a 90% accuracy rate. In order to accurately predict melanoma, Codella [7] used the ISIC 2017 dataset, which contains three kinds of skin cancer. Nevertheless, the dataset's bias and insufficient dermoscopic feature annotations led to erroneous results. For the same dataset, a different skin lesion classification instance [8] that used a suggested lesion indexing network (LIN) was able to achieve the 91.2% area under the curve. It was, however, presented at ISIC 2017, and no new

work has been produced for ISIC 2018. Moreover, some statistics categorise skin lesions into 12 separate groups. Han [9] utilised the combined 19,398 photos split into 12 categories from the Asan dataset, med-node dataset, and atlas site images. He classified data using the Resnet architecture, and his accuracy was 83%. His research also aimed to demonstrate that the suggested dataset was superior to others used for comparison. Using the HAM10000 dataset, seven different types of skin lesions, and MobileNet, Chaturvedi et al. [10] were able to detect skin lesions with an accuracy of 83%. Milton [11] introduced transfer learning techniques that used fine-tuning and freezing of two epochs and were trained on the HAM10000 dataset. PNASNet-5-Large was utilised in this study and provided an accuracy of 76%. It is more difficult to generalise the characteristics of the lesions since the HAM10000 dataset is unbalanced and has a considerable variation in the number of total images for each class. Using the HAM10000 dataset, Nugroho [17]'s own customised CNN model produced 78% accuracy. An online, non-coded method for HAM10000 illness classification and cloud training was introduced by Kadampur [16]. Although the aforementioned study works had the benefit of offering a simple algorithm approach and tolerable accuracy, the majority of them did not take into account all sorts of legions and used relatively outdated information.

Most articles classified lesions [12] into the three common types of basal cell carcinoma, squamous cell carcinoma, and melanoma, it was discovered. The classification dataset was not sufficiently large or recent to identify all forms of lesions [13].

In the last few decades, a number of strategies for melanoma classification have been presented. The majority of systems [18,19,20] extracted features from images using image processing methods, and then fed those features into a classification method. A method for melanoma and nevi detection and classification was provided by Khan et al. [21]. In order to reduce noise, the author first

used a Gaussian filter. Lesion segmentation was accomplished using K-mean clustering. Finally, using a hybrid super feature vector, textural and colour features were retrieved. Support vector machines (SVMs) were then used for categorization after that. On the ERMIS dataset, the suggested approach has a 96% accuracy rate. A novel approach based on fusing deep learning (DL) with manually created features was presented by Filali et al. [22]. Using the ISIC challenge dataset, the created approach achieved 87.8%, while on the Ph2 dataset, it achieved 98% accuracy. Hu et almethod .'s [23] was based on measuring feature similarity before classifying data with SVM. A five-layer approach called "DermoDeep" was introduced by Abbas et al. [24] to distinguish between nevi and melanoma. To get the best classification results, this strategy combined visual features with a five-layer model. Using ant-colony-based segmentation, Dalila et al. [28] retrieved three different types of characteristics (texture, geometrical attributes, and colour). ANN was then employed for categorization. In their technique, Almansour et al. [25] suggested extracting textual features before implementing SVM as a classifier. On 227 photos, the given model has a 90% accuracy rate. For the purpose of extracting ROIs, Pham et al. [26] applied image enhancement techniques. The classification of the pre-processed photos was then done using SVM. Accuracy was achieved at 87.2%. In addition to using a deep residual model to categorise the photos, Yu et al. [27] also proposed a technique to improve the images for extraction ROIs. The proposed system's attained accuracy was 85.5%.

Deep learning methods have recently been used by researchers to classify melanoma. For more accurate melanoma recognition, Yu et al. [29] developed a new strategy relying on deep CNN and feature encoding methods (FV encoding). The created model had an accuracy of 86.54% and was archived after being trained on the ISIC 2016 dataset. In order to distinguish between benign skin lesions and malignant melanoma in melanoma dermoscopy pictures, Rokhana et al. [30] suggested a deep CNN architecture. The ISIC-archive repository served as a testing ground for the proposed approach. The suggested method increased sensitivity by 91.97%, accuracy by 84.76%, and specificity by 78.71%. A classification technique based on the ensemble model was utilised by Xie et al. [35]. An ensemble model based on three classifiers was created by Liberman et al. [31] to categorise mole pictures in melanomas and non-melanomas. A novel technique based on spiking neural networks with time-dependent spike plasticity was introduced by Zhou et al. [32]. For the classification of melanoma, Hosny et al. [33] utilised a deep CNN architecture. Three different datasets were used to test the proposed technique. A CNN-based technique known as CNN malignant lesions detection was employed by Mukherjee et al (CMLD). Using the MED-NODE and Dermofit datasets, the created model has accuracy of 90.14% and 90.58%, respectively. Esteva et al. [34] presented a method for identifying skin cancer using deep networks and detecting skin disorders at an early stage.

A deep neural network-based melanoma detection model dubbed Nasnet Mobile was introduced by Cakmak et al. [36]. The HAM10000 dataset was used to evaluate the provided approach. The issue of unbalanced classes was addressed by using a variety of augmentation strategies. On the Nasnet-Mobile network, the proposed model's accuracy was 89.20 percent without data augmentation and 97.90 percent with it. ResNet50 was a pre-trained architecture that Brinker et al. [37] utilised to categorise the skin lesion as melanoma or nevi. The sensitivity and specificity ratios for the suggested model were 77.9% and 82.3%, respectively. The ResNet152 model was used by Han et al. [38] to categorise diverse skin lesions. Melanoma, seborrheic keratosis, and nevi were three separate lesions, and the specificity and mean sensitivity for each were 87.63% and 88.2%, respectively. In order to categorise skin lesions, Hosny et al. [39] swapped out the final three layers of AlexNet for fully linked layers, softmax, and an output layer. The accuracy of the suggested algorithm was 96.86%. Inception-v3 was a pre-trained model that Esteva et al. [40] utilised to categorise skin lesions. They used augmentation techniques to expand the testing dataset. The accuracy of the suggested classification model was 71.2%.

PROPOSED ARCITECTURE

Artificial intelligence's core is built on self-learning algorithms. Such algorithms continue to change as new information about the job is acquired. To address these challenges, these techniques are always developing. Because these models are based on the human brain, self-learning algorithms can work. Similar to human brain cells, artificial neural networks (ANNs) are made up of nodes (neurons) that are coupled at different levels. Inside this neuron network, information is input, processed (through positive or negative weighting), and output. Because they have several layers and can recognise more intricate patterns, ANNs appear to be particularly promising. The learning processes that these networks are capable of are referred to as "deep learning".

In order to categorise skin cancer melanoma, this study introduces a deep transfer learning method. Pre-processing and other augmentation techniques are utilised at the first level to generate diversity and address the problem of class imbalance in the dataset. A pre-trained "MobileNetV2" model is used to identify the malignant melanoma from a benign skin lesion at the second level after auto characteristics are retrieved. Figure 1 shows the flow chart for the suggested technique.

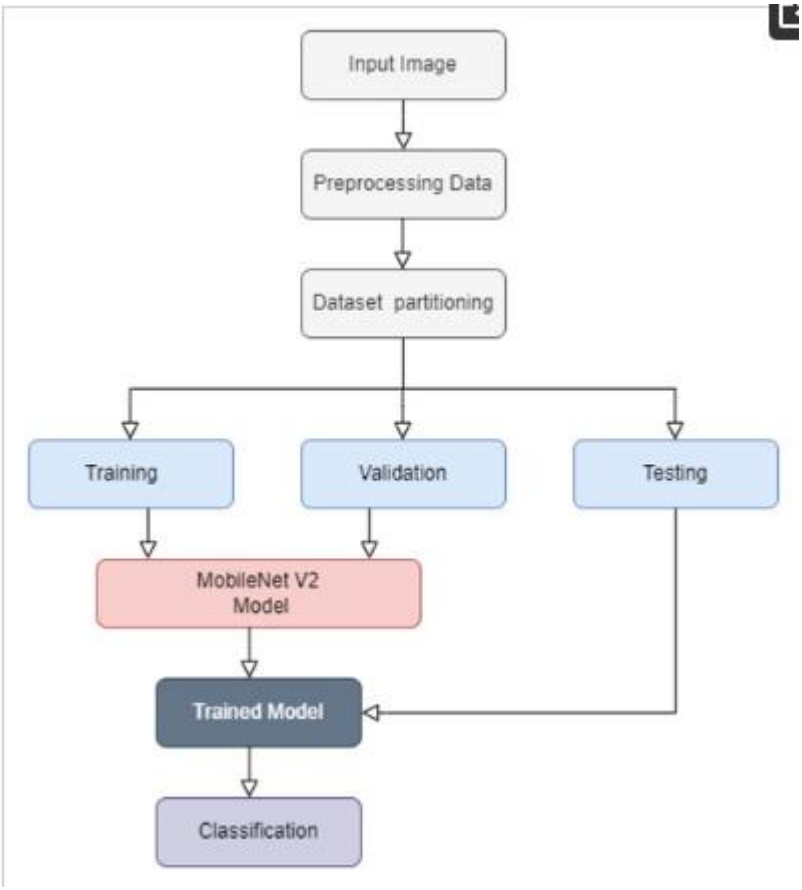

FIGURE-1 PROPOSED METHOD FLOWCHART

Dataset

The effectiveness of deep learning techniques depends on a valid and appropriate dataset being available. The research in question makes use of the following dataset.

Dataset SIIM-ISIC 2020

The world's largest collection of quality-controlled dermoscopic pictures of skin lesions is available for research in the ISIC-2020 Archive. Data from patients of all ages and sexual orientations were supplied by several institutes. The dataset contains 32,542 benign skin lesions and 33,126 dermoscopic photos from more than 2000 patients, together with 584 images of malignant skin lesions. An individual patient identification links each image to one of these patients. 584 pictures of melanoma and 11,670 photos of benign class were used. Taking into

account how the data for these two classes is biassed. Hence, 4522 melanoma photos were added to the ISIC 2019 archive in order to address the issue of the class imbalance. The data was then subjected to a number of data augmentation techniques, including rescaling, width shift, rotation, shear range, horizontal flip, and channel shift, and the final result was 11,670 after augmentation. To address the topic of class inequality, 11,670 photos of kids were used. Out of the entire collection of photos, the photographs belonging to the innocuous class were randomly chosen. See sample photos in Figure 2.

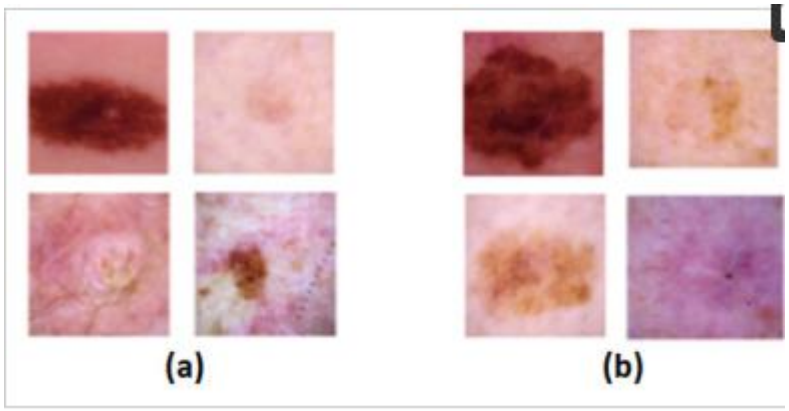

Figure-2

Pre-processing of Images

Preprocessing is used for all of the input images of the ISIC-2020 in order to get classification results that are more consistent and have better features. A large-scale image dataset was needed for the CNN approach's massively repetitive training in order to avoid the risk of over-fitting.

Image Resizing

The original ISIC dataset includes 6000 4000-pixel versions of each image. the dataset is resized to 256 X 256. The model performance will be drastically reduced, and the processing time will be sped up.

Data Augmentation

With the aid of the Python image data generator function of the Keras library, various data augmentation techniques have been applied to the training set to reduce overfitting and boost the dataset's variety. Scale transformation was used

to reduce the computational cost by using smaller pixel values within the same range. Consequently, using the parameter value (1. /255), the value of each pixel ranged from 0 to 1. The photos were rotated to a specific angle using the rotation transformation; as a result, 25 degrees was used to rotate the photographs. By using the width shift range transformation, images can be moved freely to the right or left; the width shift parameter was set to 0.1. The height shift range option was utilised to vertically shift the training images with a value of 0.1.Shear transformation is a method that fixes one axis of a image while stretching the other axis at a predetermined angle, in this case, a 0.2 shear angle. The random zoom transformation was done using the zoom range argument; a value larger than 1.0 indicates that the photos were zoomed in, and a value less than 1.0 indicates that they were zoomed out. As a result, the image was enlarged using a 0.2 zoom range. The image was horizontally flipped using the flip tool. The zoom range was set to 0.5–1.0 using brightness transformation, where 0.0 denotes no brightness and 1.0 denotes maximum brightness. The 0.05 channel shift range was used, and the fill mode was the closest because in channel shift transformation, the channel values are randomly shifted by a random value selected from the specific range.

Tests, Validation, and Training

Training, testing, and validation sections made up the ISIC-2020 dataset. The MobileNetV2 model was trained using the training dataset, and its performance was assessed using the validation and test datasets. As a result, we divided the dataset into training, testing, and validation, with respective weights of 70%, 15%, and 15%. In order to train the MobileNetV2 model, the dataset was used. 16,350, 3500, and 3500 photos were used for the ISIC-2020 dataset's training, validation, and testing, respectively.

MobileNetV2 Architecture

Deep transfer learning MobileNetV2 architecture will be used in the current study to address the problem of melanoma classification. The choice of the MobileNetV2 model was influenced by a number of distinct considerations. A modest but more expressive system, like MobileNetV2, greatly reduced the over-fitting effect that could have been caused by the very short dataset utilised for model training. With regard to the error, MobileNetV2 is a framework that optimises execution speed and memory use at the lowest possible cost. High execution speed makes parameter customization and experimentation much

easier to manage, and low memory consumption is another appealing quality. MobileNetV2's fundamental architecture is based on that of MobileNetV1, its predecessor. The depthwise separable convolution, linear bottleneck, and inverted residual are three key ideas that contribute to the explanation of the MobileNetV2 framework and are further explained.

Deeply Separable Convolutions

Additional effective networks employ the depthwise separable convolution, such ShuffleNet and Xception. In MobileNetV2, the Depthwise separable convolution that was employed in MobileNetV1 was also utilised. Traditional convolution is replaced by two processes called depth-wise separable convolution. Each feature map is subjected to a distinct convolution in the first procedure, which is known as a features map-wise convolution. The feature maps produced by this technique are stacked before being processed using the second procedure, a pointwise convolution. In this instance, a 1 X 1 kernel is used to implement pointwise convolution across all feature maps simultaneously. According to Figure 3, the image is convolutionally processed simultaneously in its height, breadth, and channel dimensions. However, the depthwise separable convolution analyzes the image by height and width dimensions during the first procedure. It handles the channel dimensions during the second procedure, which refers to a factorization of the traditional convolution.

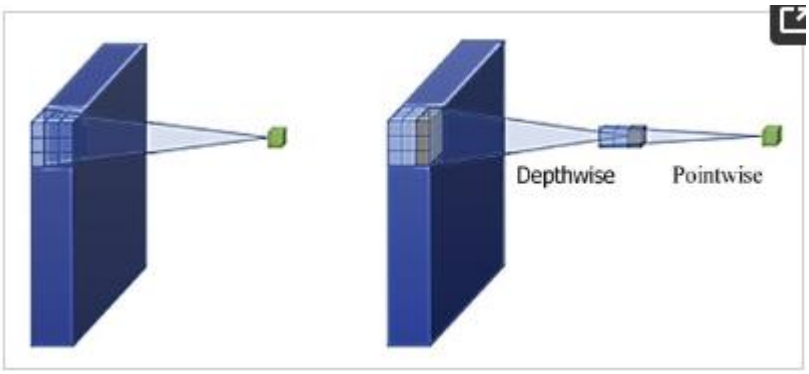

Figure-3 Traditional convolution and depth-wise separable convolution.

Means of Assessment for Classification

The suggested method was evaluated on the testing dataset following the training procedure. The accuracy, F1 score, precision, and recall were used to verify the performance of the architecture. Here is a detailed examination of the performance metrics used in this study. Here are the definitions and equations, where TP denotes true positives, TN denotes true negatives, FN denotes false negatives, and FP denotes false positives.

Classification Accuracy

The proportion of accurate predictions to all accurate predictions is used to calculate the classification accuracy.

$$\text{Accuracy} = \frac{\text{TP} + \text{TN}}{(\text{TP} + \text{TN} + \text{FP} + \text{FN})}$$

Precision

Classification accuracy is not always a reliable indicator of overall model performance, as shown by a number of examples. One of these situations is when there is an uneven distribution of classes. It makes no sense to attain a high accuracy rate if we treat all samples as being of the greatest calibre. Contrarily, accuracy implies that consistency can be established when using the same instrument again, such as when measuring the same part. One of these metrics is precision, which is defined as

$$\text{Precision} = \frac{\text{TP}}{(\text{TP} + \text{FP})}$$

Recall

A recall is another vital statistic, which can be defined as dividing input samples into classes that are successfully predicted by the system. The recall is calculated as

$$\text{Recall} = \frac{\text{TP}}{(\text{TP} + \text{FN})}$$

F1 Score

The f1 score is a well-known metric that measures precision and recall in a single metric. The f1 score is calculated as

$$\text{F1 Score} = \frac{2 * (\text{Precision} * \text{Recall})}{(\text{Precision} + \text{Recall})}$$

ROC Curve and AUC Score

The receiver operating characteristic (ROC), which is a probability curve, and the area under curves (AUC), which measure the degree of separability. The relationship between specificity (rate of false positives) and sensitivity is shown in a graph by the ROC curve (true positive rate).

RESULTS AND ANALYSIS

BASE MODEL VGG19:

Transfer learning is a great way to reap the benefits of a well-trained model without having the train the model ourselves. Since VGG16 has already been trained, we do not change the weights in this model and set its ```trainable``` attribute to ```False```. We also don't want to include the top layers because the classification that we want to accomplish in this model is not the same as the classification that the model was originally trained on. We want the a single node output that determines the probability that the lesion will be malignant.

However, because the data is imbalanced, this model will not work very well.

In [20]:
```
def make_model(output_bias = None, metrics = None):
    if output_bias is not None:
        output_bias = tf.keras.initializers.Constant(output_bias)

    base_model = tf.keras.applications.Xception(input_shape=(*IMAGE_RESIZE, 3),
                                                include_top=False,
                                                weights='imagenet')

    base_model.trainable = False

    model = tf.keras.Sequential([
        base_model,
        tf.keras.layers.GlobalAveragePooling2D(),
        tf.keras.layers.Dense(8, activation='relu'),
        tf.keras.layers.Dense(1, activation='sigmoid',
                              bias_initializer=output_bias)
    ])

    model.compile(optimizer='adam',
                  loss='binary_crossentropy',
                  metrics=metrics)

    return model
```

In [21]:
```
STEPS_PER_EPOCH = NUM_TRAINING_IMAGES // BATCH_SIZE
VALID_STEPS = NUM_VALIDATION_IMAGES // BATCH_SIZE
```

Correcting for data imbalance:

Set initial bias

Set the correct initial bias for our model so it doesn't waste time figuring out that there are not many malignant images in our dataset. We want our output layer to reflect the imbalance that we have in our data.

In [22]:
```
initial_bias = np.log([malignant/benign])
initial_bias
```

Out[22]:
```
array([-4.02038586])
```

Set initial bias

Set the correct initial bias for our model so it doesn't waste time figuring out that there are not many malignant images in our dataset. We want our output layer to reflect the imbalance that we have in our data.

In [23]:
```
weight_for_0 = (1 / benign)*(total_img)/2.0
weight_for_1 = (1 / malignant)*(total_img)/2.0

class_weight = {0: weight_for_0, 1: weight_for_1}

print('Weight for class 0: {:.2f}'.format(weight_for_0))
print('Weight for class 1: {:.2f}'.format(weight_for_1))
```

```
Weight for class 0: 0.51
Weight for class 1: 28.36
```

Deciding our evaluation metrics

Due to initial data imbalance and the fact that it is riskier to predict a malignant tumor as benign than it is to predict a benign tumor as malignant, accuracy alone cannot be our metric. Thus, the area under the ROC curve is used.

In [24]:
```
with strategy.scope():
    model = make_model(output_bias = initial_bias, metrics=tf.keras.metrics.AUC(name='auc'))
```

```
Downloading data from https://storage.googleapis.com/tensorflow/keras-applications/xception/xception_weights_tf_dim_ordering_tf_kernels_notop.h5
83689472/83683744 [==============================] - 0s 0us/step
```

We can use callbacks to stop training when there are no improvements in our validation set predictions, and this stops overfitting. Additionally, we can save the best weights for our model so that it doesn't have to be retrained. At the end of the training process, the model will restore the weights of its best iteration.

In [25]:
```
checkpoint_cb = tf.keras.callbacks.ModelCheckpoint("melanoma_model.h5",
                                                   save_best_only=True)

early_stopping_cb = tf.keras.callbacks.EarlyStopping(patience=10,
                                                     restore_best_weights=True)
```

In [26]:
```
history = model.fit(
    train_dataset, epochs=100,
    steps_per_epoch=STEPS_PER_EPOCH,
    validation_data=valid_dataset,
    validation_steps=VALID_STEPS,
    callbacks=[checkpoint_cb, early_stopping_cb, lr_scheduler],
    class_weight=class_weight
)
```

```
Epoch 1/100
226/226 [==============================] - 72s 319ms/step - loss: 0.6084 - auc: 0.7699 - val_loss: 0.3363 - val_auc: 0.7408
- lr: 0.0100
Epoch 2/100
226/226 [==============================] - 45s 198ms/step - loss: 0.4998 - auc: 0.8383 - val_loss: 0.2864 - val_auc: 0.7296
- lr: 0.0089
Epoch 3/100
226/226 [==============================] - 41s 183ms/step - loss: 0.4673 - auc: 0.8639 - val_loss: 0.1685 - val_auc: 0.7607
```

The probability that a tumor is malignant based on the image of the lesion using our testing dataset.

	image_name	target
0	ISIC_0052060	0.017053
1	ISIC_0052349	0.019425
2	ISIC_0058510	0.017053
3	ISIC_0073313	0.017053
4	ISIC_0073502	0.017053

CONTRIBUTION

NAMES	WORK
MIZBA K	Data pre processing, normalizing, extracting label, Debugging
POULAMI BERA	Data augmentation, VGG16 model , potser making, code debugging
RASHIKA AGARWAL	Report paper, result and analysis and performance matrices, research work

CONCLUSION

The most dangerous kind of skin cancer is melanoma, although if detected early enough, it may not be fatal. Thus, it is crucial to use complementary imaging modalities that have been shown to aid in diagnosis. These techniques were developed by medical professionals to find melanoma before it spread to neighbouring lymph nodes. In this study, we provide a MobileNetV2-based transfer learning model for the identification of benign and malignant skin lesions that can be used to examine any suspected lesion. The recommended approach is used to classify diseases as benign or malignant using photos of skin cancer disorders from an ISIC2020 challenge dataset. Techniques for data augmentation were employed to expand the dataset and enhance MobileNetV2's precision. This design has a diagnosis accuracy of 98.2 percent and performs well. Lastly, the suggested framework is used to compare the accuracy of various state-of-the-art models. The proposed architecture was found to offer exceptional classification accuracy without the need for model retraining to increase model

REFRENCES-:

[1]. Voulodimos A., Doulamis N., Doulamis A., Protopapadakis E. Deep Learning for Computer Vision: A Brief Review. *Comput. Intell. Neurosci.* 2018;**2018**:7068349. doi: 10.1155/2018/7068349. [PMC free article] [PubMed] [CrossRef] [Google Scholar]

[2]. Guo Y., Liu Y., Oerlemans A., Lao S., Wu S., Lew M.S. Deep learning for visual understanding: A review. *Neurocomputing.* 2016;**187**:27–48. doi: 10.1016/j.neucom.2015.09.116. [CrossRef] [Google Scholar]

[3]. Garcia-Garcia A., Orts-Escolano S., Oprea S., Villena-Martinez V., Garcia-Rodriguez J. A Review on Deep Learning Techniques Applied to Semantic Segmentation. [(accessed on 1 April 2017)];*arXiv.* 2017 Available online: https://ui.adsabs.harvard.edu/abs/2017arXiv170406857G1704.06857 [Google Scholar]

[4]. Maheshwari K., Shaha A., Arya D., Rajasekaran R., Tripathy B.K. Deep Learning: Research and Applications. In: Siddhartha B., Vaclav S., Aboul Ella H., Satadal S., Tripathy B.K., editors. *Convolutional Neural Networks: A Bottom-Up Approach.* De Gruyter; Berlin, Germany: 2020. pp. 21–50. [CrossRef] [Google Scholar]

[5]. Mateen M., Wen J., Nasrullah, Song S., Huang Z. Fundus Image Classification Using VGG-19 Architecture with PCA and SVD. *Symmetry*. 2019;**11**:1. doi: 10.3390/sym11010001. [CrossRef] [Google Scholar]

[6]. Canziani A., Paszke A., Culurciello E. An Analysis of Deep Neural Network Models for Practical Applications. *arXiv.* 20161605.07678 [Google Scholar]

[7]. Codella N.C.F., Gutman D., Celebi M.E., Helba B., Marchetti M.A., Dusza S.W., Kalloo A., Liopyris K., Mishra N., Kittler H., et al. Skin lesion analysis toward melanoma detection: A challenge at the 2017 International symposium on biomedical imaging (ISBI), hosted by the international skin imaging collaboration (ISIC); Proceedings of the 2018 IEEE 15th International Symposium on Biomedical Imaging (ISBI 2018); Washington, DC, USA. 4–7 April 2018; pp. 168–172. [Google Scholar]

[8]. Li Y., Shen L. Skin Lesion Analysis towards Melanoma Detection Using Deep Learning Network. *Sensors.* 2018;**18**:556. doi: 10.3390/s18020556. [PMC free article] [PubMed] [CrossRef] [Google Scholar]

[9]. Han S.S., Kim M.S., Lim W., Park G.H., Park I., Chang S.E. Classification of the Clinical Images for Benign and Malignant Cutaneous Tumors Using a Deep Learning Algorithm. *J. Investig. Dermatol.* 2018;**138**:1529–1538. doi: 10.1016/j.jid.2018.01.028. [PubMed] [CrossRef] [Google Scholar]

[10]. Chaturvedi S.S., Gupta K., Prasad P.S. Skin Lesion Analyser: An Efficient Seven-Way Multi-class Skin Cancer Classification Using MobileNet. *Adv. Mach. Learn. Technol. Appl.* 2020;**1141**:165–176. doi: 10.1007/978-981-15-3383-9_15. [CrossRef] [Google Scholar]

[11]. Milton M.A.A. Automated Skin Lesion Classification Using Ensemble of Deep Neural Networks in ISIC 2018: Skin Lesion Analysis Towards Melanoma Detection Challenge. *arXiv.* 20191901.10802 [Google Scholar]

[12]. Esteva A., Kuprel B., Novoa R.A., Ko J., Swetter S.M., Blau H.M., Thrun S. Dermatologist-level classification of skin cancer with deep neural networks. *Nature.* 2017;**542**:115–118. doi: 10.1038/nature21056. [PMC free article] [PubMed] [CrossRef] [Google Scholar]

[13]. Goyal M., Oakley A., Bansal P., Dancey D., Yap M.H. Skin Lesion Segmentation in Dermoscopic Images With Ensemble Deep Learning Methods. *IEEE Access.* 2020;**8**:4171–4181. doi: 10.1109/ACCESS.2019.2960504. [CrossRef] [Google Scholar]

[14]. Farooq A., Jia X., Hu J., Zhou J. Transferable Convolutional Neural Network for Weed Mapping With Multisensor Imagery. *IEEE Trans. Geosci. Remote Sens.* 2021:1–16. doi: 10.1109/TGRS.2021.3102243. [CrossRef] [Google Scholar]

[15]. Farooq A., Jia X., Hu J., Zhou J. Knowledge Transfer via Convolution Neural Networks for Multi-Resolution Lawn Weed Classification; Proceedings of the 2019 10th Workshop on Hyperspectral Imaging and Signal Processing: Evolution in Remote Sensing (WHISPERS); Amsterdam, The Netherlands. 24–26 September 2019; pp. 1–5. [Google Scholar]

[16]. Kadampur M.A., Al Riyaee S. Skin cancer detection: Applying a deep learning based model driven architecture in the cloud for classifying dermal cell images. *Inform. Med. Unlocked.* 2020;**18**:100282. doi: 10.1016/j.imu.2019.100282. [CrossRef] [Google Scholar]

[17]. Nugroho A.A., Slamet I., Sugiyanto Skins cancer identification system of HAMl0000 skin cancer dataset using convolutional neural network. *AIP Conf. Proc.* 2019;**2202**:020039. doi: 10.1063/1.5141652. [CrossRef] [Google Scholar]

[18]Giotis, I.; Molders, N.; Land, S.; Biehl, M.; Jonkman, M.F.; Petkov, N. MED-NODE: A computer-assisted melanoma diagnosis system using non-dermoscopic images. *Expert Syst. Appl.* **2015**, *42*, 6578–6585. [**Google Scholar**] [**CrossRef**]

[19]Lynn, N.C.; War, N. Melanoma classification on dermoscopy skin images using bag tree ensemble classifier. In Proceedings of the 2019 International Conference on Advanced Information Technologies (ICAIT), Yangon, Myanmar, 6–7 November 2019; pp. 120–125. [**Google Scholar**]

[20]Mukherjee, S.; Adhikari, A.; Roy, M. Melanoma identification using MLP with parameter selected by metaheuristic algorithms. In *Intelligent Innovations in Multimedia Data Engineering and Management*; IGI Global: Hershey, PA, USA, 2019; pp. 241–268. [**Google Scholar**]

[21]Khan, M.Q.; Hussain, A.; Rehman, S.U.; Khan, U.; Maqsood, M.; Mehmood, K.; Khan, M.A. Classification of melanoma and nevus in digital images for diagnosis of skin cancer. *IEEE Access* **2019**, *7*, 90132–90144. [**Google Scholar**] [**CrossRef**]

[22]Filali, Y.; El Khoukhi, H.; Sabri, M.A.; Aarab, A. Efficient fusion of handcrafted and pre-trained CNNs features to classify melanoma skin cancer. *Multimed. Tools Appl.* **2020**, *79*, 31219–31238. [**Google Scholar**] [**CrossRef**]

[23]Hu, K.; Niu, X.; Liu, S.; Zhang, Y.; Cao, C.; Xiao, F.; Yang, W.; Gao, X. Classification of melanoma based on feature similarity measurement for codebook learning in the bag-of-features model. *Biomed. Signal Process. Control* **2019**, *51*, 200–209. [**Google Scholar**] [**CrossRef**]

[24]Abbas, Q.; Celebi, M.E. DermoDeep-A classification of melanoma-nevus skin lesions using multi-feature fusion of visual features and deep neural network. *Multimed. Tools Appl.* **2019**, *78*, 23559–23580. [**Google Scholar**] [**CrossRef**]

[25]Almansour, E.; Jaffar, M.A. Classification of Dermoscopic skin cancer images using color and hybrid texture features. *IJCSNS Int. J. Comput. Sci. Netw. Secur.* **2016**, *16*, 135–139. [**Google Scholar**]

[26]Pham, T.C.; Luong, C.M.; Visani, M.; Hoang, V.D. Deep CNN and data augmentation for skin lesion classification. In *Asian Conference on Intelligent Information and Database Systems*; Springer: Berlin/Heidelberg, Germany, 2018; pp. 573–582. [**Google Scholar**]

[27]Yu, L.; Chen, H.; Dou, Q.; Qin, J.; Heng, P.A. Automated melanoma recognition in dermoscopy images via very deep residual networks. *IEEE Trans. Med. Imaging* **2016**, *36*, 994–1004. [**Google Scholar**] [**CrossRef**]

[28]Dalila, F.; Zohra, A.; Reda, K.; Hocine, C. Segmentation and classification of melanoma and benign skin lesions. *Optik* **2017**, *140*, 749–761. [**Google Scholar**] [**CrossRef**]

[29]Yu, Z.; Jiang, X.; Zhou, F.; Qin, J.; Ni, D.; Chen, S.; Lei, B.; Wang, T. Melanoma recognition in dermoscopy images via aggregated deep convolutional features. *IEEE Trans. Biomed. Eng.* **2018**, *66*, 1006–1016. [**Google Scholar**] [**CrossRef**]

[30]Rokhana, R.; Herulambang, W.; Indraswari, R. Deep convolutional neural network for melanoma image classification. In Proceedings of the 2020 International Electronics Symposium (IES), Marrakech, Morocco, 24–26 March 2020; pp. 481–486. [**Google Scholar**]

[31]]Liberman, G.; Acevedo, D.; Mejail, M. Classification of melanoma images with fisher vectors and deep learning. In *Iberoamerican Congress on Pattern Recognition*; Springer: Berlin/Heidelberg, Germany, 2018; pp. 732–739. [**Google Scholar**]

[32]Zhou, Q.; Shi, Y.; Xu, Z.; Qu, R.; Xu, G. Classifying melanoma skin lesions using convolutional spiking neural networks with unsupervised stdp learning rule. *IEEE Access* **2020**, *8*, 101309–101319. [**Google Scholar**] [**CrossRef**]

[33]Hosny, K.M.; Kassem, M.A.; Foaud, M.M. Skin melanoma classification using ROI and data augmentation with deep convolutional neural networks. *Multimed. Tools Appl.* **2020**, *79*, 24029–24055. [**Google Scholar**] [**CrossRef**]

[34]Esteva, A.; Kuprel, B.; Thrun, S. *Deep Networks for Early Stage Skin Disease and Skin Cancer Classification*; Stanford University: Stanford, CA, USA, 2015. [**Google Scholar**]

[35]Xie, F.; Fan, H.; Li, Y.; Jiang, Z.; Meng, R.; Bovik, A. Melanoma classification on dermoscopy images using a neural network ensemble model. *IEEE Trans. Med. Imaging* **2016**, *36*, 849–858. [**Google Scholar**] [**CrossRef**]

[36]Çakmak, M.; Tenekecı, M.E. Melanoma detection from dermoscopy images using Nasnet Mobile with Transfer Learning. In Proceedings of the 2021 29th Signal Processing and Communications Applications Conference (SIU), Istanbul, Turkey, 9–11 June 2021; pp. 1–4. [**Google Scholar**]

[37]Brinker, T.J.; Hekler, A.; Enk, A.H.; Berking, C.; Haferkamp, S.; Hauschild, A.; Weichenthal, M.; Klode, J.; Schadendorf, D.; Holland-Letz, T.; et al. Deep neural networks are superior to dermatologists in melanoma image classification. *Eur. J. Cancer* **2019**, *119*, 11–17. [**Google Scholar**] [**CrossRef**][**Green Version**]

[38]Han, S.S.; Kim, M.S.; Lim, W.; Park, G.H.; Park, I.; Chang, S.E. Classification of the clinical images for benign and malignant cutaneous tumors using a deep learning algorithm. *J. Investig. Dermatol.* **2018**, *138*, 1529–1538. [**Google Scholar**] [**CrossRef**] [**PubMed**][**Green Version**]

[39]Hosny, K.M.; Kassem, M.A.; Foaud, M.M. Classification of skin lesions using transfer learning and augmentation with Alex-net. *PLoS ONE* **2019**, *14*, e0217293. [**Google Scholar**] [**CrossRef**] [**PubMed**][**Green Version**]

[40]Esteva, A.; Kuprel, B.; Novoa, R.A.; Ko, J.; Swetter, S.M.; Blau, H.M.; Thrun, S. Dermatologist-level classification of skin cancer with deep neural networks. *Nature* **2017**, *542*, 115–118. [**Google Scholar**] [**CrossRef**] [**PubMed**]